$FeAl_2O_4$–$MgAl_2O_4$: Growth and Some Thermal, Optical, and Magnetic Properties of Mixed Single Crystals

GLEN A. SLACK
General Electric Research Laboratory, Schenectady, New York
(Received 30 December 1963)

Synthetic single crystals of $FeAl_2O_4$ have been grown from the melt. Measurements of the thermal conductivity K and optical absorption coefficient α have been made on a combination of synthetic and natural single crystals of $Mg_{1-x}Fe_xAl_2O_4$ for $0 \leq x \leq 1$. The α measurements at 300°K in the absorption band of tetrahedral Fe^{2+} between 0.4 and 0.6 eV have been calibrated and then used to measure x. The thermal conductivity results between 3 and 300°K show that the heat is conducted by phonons and that tetrahedral Fe^{2+} is a very effective phonon scatterer at all temperatures because it possesses a series of low-lying energy levels in the $3d$ shell. This type of scattering is absent in $CoAl_2O_4$. The phonon scattering by Fe^{2+} is dominant for $x>0.1$, and for these crystals $K \sim T/\sqrt{x}$. The magnetic susceptibility χ of a single crystal of $FeAl_2O_4$, measured between 2 and 290°K, shows a peak at 9.5±0.5°K. The analysis of the χ and K measurements suggests that the ~10°K transition is caused by the individual Fe^{2+} ions, and is not associated with a long-range, antiferromagnetic ordering of the $FeAl_2O_4$.

INTRODUCTION

THE simplest magnetic analog of the basic diamagnetic spinel $MgAl_2O_4$ is one in which all or part of the Mg is replaced by a transition-metal ion M. The present series of studies concerns crystals in which M is divalent Fe. The compound $FeAl_2O_4$ is a normal spinel[1,2] as is[3,4] $MgAl_2O_4$ in which almost all of the Fe (or Mg) ions are in the tetrahedral (or A) lattice sites. The magnetic properties in a completely normal spinel are thus determined by the magnetic A-A interaction. Since the A-A separation is 3.52 Å in $FeAl_2O_4$, this interaction is very weak.[5] Thus, it is not possible for $FeAl_2O_4$ to become magnetically ordered until very low temperatures (~ 4°K) are reached. The following measurements at and below 300°K of the thermal conductivity, optical absorption, and magnetic susceptibility of synthetic single crystals of $FeAl_2O_4$ and of natural mixed crystals of $Mg_{1-x}Fe_xAl_2O_4$ give some information on the behavior of the individual Fe ions and some on the nature of the A-A interaction.

SINGLE CRYSTALS

The samples used in the present study were a combination of synthetic and natural crystals. See Table I. High-purity oligocrystalline $MgAl_2O_4$ prepared[6] by Navias by the vapor reaction of MgO with Al_2O_3 was used as a comparison standard. A large sample 1.2×0.3 ×0.3 cm composed of about five single crystals was obtained, and was used for the thermal conductivity and optical absorption measurements. A combination of chemical and x-ray analyses indicated this sample, R68, was a nearly stoichiometric spinel with a composition, 1 MgO+1.02 Al_2O_3, slightly rich in Al_2O_3. The crystallite diameter of 0.3 cm is sufficiently large so that these results should be representative of single-crystal values.

Natural crystals of $Mg_{1-x}Fe_xAl_2O_4$, where $0.0005 \leq x \leq 0.3$ were obtained through various sources. They originated in Australia (Queensland), Burma, and Ceylon. For the lowest values of x they were light pink in color. This color is caused by the presence of Cr in these, as in almost all natural spinel samples. For $x=0.3$, the crystals were opaque black in the massive state, but in thin, polished sections were a yellowish-brown color.

No good natural crystals of hercynite, $FeAl_2O_4$, were available. Therefore synthetic single crystals of $FeAl_2O_4$ were grown from the melt in an iridium crucible under a controlled partial pressure of oxygen.

$FeAl_2O_4$ Crystals

Since single crystals of $FeAl_2O_4$ do not appear to have been grown before, it seems worthwhile to describe their preparation. The FeO-Al_2O_3 phase diagram at high temperatures has been worked out by Fischer and

TABLE I. A list of the single crystals of $Mg_{1-x}Fe_xAl_2O_4$ used in the present studies.

Sample number	a_0 Å	x[a]	Source	Color
R68	8.082	3×10^{-5}	synthetic	colorless in bulk
R42	8.0866	5×10^{-4}	Burma	light pink in bulk
R54	8.0868	6.0×10^{-4}	Burma	light pink in bulk
R97	8.089	2.4×10^{-2}	Ceylon	bluish purple in bulk
R56	8.128	1.9×10^{-1}	Australia	opaque, yellowish-brown thin sections
R62	8.117	2.7×10^{-1}	Australia	opaque, yellowish-brown thin sections
R67	8.138	~1.0	synthetic	opaque, greenish-yellow in thin sections
R75	8.140	~1.0	synthetic	opaque, greenish-yellow in thin sections

[a] x = fraction of the A sites occupied by Fe^{2+} ions as determined from the 0.6 eV optical absorption peak. For sample R68 the Fe concentration was determined from an emission spectrograph.

[1] T. W. F. Barth and E. Posnjak, Z. Krist. **82**, 325 (1932).
[2] F. C. Romeijn, Philips Res. Rept. **8**, 304, 321 (1953).
[3] G. E. Bacon, Acta Cryst. **5**, 684 (1952).
[4] S. Hafner and F. Laves, Z. Krist. **115**, 321 (1961).
[5] W. Roth, Proceedings of the International Colloquium of Neutron Diffusion and Diffraction, Grenoble, 1963 (unpublished); J. Phys. Radium (to be published).
[6] L. Navias, J. Am. Ceram. Soc. **44**, 434 (1961).

Hoffmann[7] and by Galakhov.[8] They show that $FeAl_2O_4$ is the only ternary compound in the system, and it has a congruent melting point between 1780 and 1800°C. The partial pressure of oxygen at the phase boundary where $FeAl_2O_4$ dissociates into Fe, Al_2O_3, and O_2 has been measured[9–12] between 900 and 1100°C. When these data are extrapolated to the melting point at 1780°C, the predicted dissociation pressure is 10^{-7} atm of oxygen. A gas mixture of carbon monoxide to carbon dioxide in a molecular ratio of 8 to 1 at a total pressure in the vicinity of 1 atm will possess[13] this partial pressure of oxygen at 1780°C. Such an 8 to 1 mixture will provide an oxygen pressure about 5 times the dissociation pressure at 1000°C. Thus, a CO/CO_2 gas mixture of constant composition is a nearly ideal medium to use for growing $FeAl_2O_4$ since it will supply an oxygen partial pressure very close to the one needed. If the oxygen partial pressure becomes too high, much of the Fe^{2+} will be converted to the unwanted Fe^{3+}. The major problem in making $FeAl_2O_4$ is to keep as much of the iron as possible in the divalent Fe^{2+} state. In analogy with wüstite, "FeO," it may never be possible to have all of the iron in the divalent state.[14]

The $FeAl_2O_4$ crystals were therefore grown in a CO/CO_2 atmosphere with a molecular ratio of 1 part CO to 1 part CO_2. This is slightly more oxidizing than necessary in order to provide a margin of safety. Following the work of Horn[15] on ferrites, crucibles of pure iridium were used. These were in the shape of a tapered cylinder with a conical end to facilitate growth of only a few nuclei. The crystal growing furnace is shown in Fig. 1. The iridium crucible is placed inside of an iridium cylinder with a 0.05 cm wall thickness which acts as an rf susceptor. The heat is supplied by a 0.5-Mc, 25-kW radiofrequency oscillator. The rf coil, 20 cm long, is wound with a change in diameter and pitch at its midpoint, as shown in Fig. 1. The operating power level is adjusted so that the $FeAl_2O_4$ in the crucible is liquid when the crucible is in the upper part of the rf coil, and is solid when in the lower part. The temperature difference between the two parts of the coil is approximately 300°C. The motion of the temperature gradient in this modified Bridgman technique is produced by moving the rf coil upward past the crucible at a rate of 1 cm/h. After the melt has solidified, the power level of the rf oscillator is slowly reduced to zero over a period of hours. The thermal insulation around the iridium susceptor was composed of zirconia ceramic, Pt-40% Rh radiation shields, alumina ceramic, and quartz. Most of this detail has been omitted from Fig. 1. for clarity.

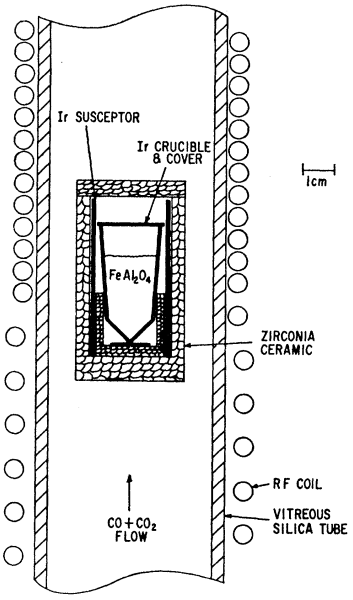

FIG. 1. A schematic of the apparatus used for growing single crystals of $FeAl_2O_4$ by a modified Bridgman technique. The rf coil is moved upward past the stationary crucible.

Large, sound single crystals of the order of 1 cm^3 in volume were produced by this technique. Metallographic and x-ray analyses indicated a single-phase material with the spinel-crystal structure and a lattice parameter a_0 of 8.138±0.001 Å for the as-grown sample R67. This value for a_0 is in reasonable agreement with the literature values[5,16–22] listed in Table II. It appears to be somewhat smaller than the most recent values on samples equilibrated at 1000°C, which cluster around 8.151 Å. If the results of Holgersson[16] on a natural crystal are corrected for the small concentration of $MgAl_2O_4$ in his sample, one obtains 8.155±0.004 Å. The variation in a_0 of a nominally pure $FeAl_2O_4$ sample can be caused[20,22] by the formation of mixed crystals with Al_2O_3, which reduces a_0, or with Fe_3O_4, which increases a_0. It can also be caused by a partial inversion[5,22] of the spinel from its ideal normal structure, or by oxidation of some Fe^{2+} to Fe^{3+}.

A chemical analysis of the as-grown crystal R67

[7] W. A. Fischer and A. Hoffmann, Arch. Eisenhüttenw. **27**, 344 (1956).
[8] F. Ya. Galakhov, Izvest. Akad. Nauk SSSR, Otd. Khim. Nauk (1957), p. 525.
[9] R. Schenk, H. Franz, H. Willeke, Z. Anorg. Allgem. Chem. **184**, 1 (1929).
[10] V. Cirilli, Gazz. Chim. Ital. **76**, 339 (1946).
[11] F. D. Richardson, J. H. E. Jeffres, G. Withers, J. Iron Steel Inst. (London) **166**, 213 (1950).
[12] R. G. Richards and J. White, Trans. Brit. Ceram. Soc. **53**, 233 (1954).
[13] F. D. Richardson and J. H. E. Jeffres, J. Iron Steel Inst. (London) **160**, 261 (1948).
[14] L. S. Darken and R. W. Gurry, J. Am. Chem. Soc. **67**, 1398 (1945).
[15] F. H. Horn, J. Appl. Phys. **32**, 900 (1961).
[16] S. Holgersson, Lunds Univ. Arsskr. Adv. 2 **38**, 1 (1927); Chem. Abstr. **24**, 804 (1930).
[17] G. L. Clark, A. Ally, A. E. Badger, Am. J. Sci. **22**, 539 (1931).
[18] O. Krause and W. Thiel, Z. Anorg. Allgem. Chem. **203**, 120 (1931).
[19] H. Tazaki and S. Kuwabara, J. Sci. Hiroshima Univ. **A15**, 263 (1952).
[20] A. Hoffmann and W. A. Fischer, Z. Physik. Chem. (Frankfurt) **7**, 80 (1956).
[21] L. M. Atlas and W. K. Sumida, J. Am. Ceram. Soc. **41**, 150 (1958).
[22] A. C. Turnock, Carnegie Inst. Wash. Year Book **58**, 134 (1958).

TABLE II. Values for the x-ray lattice constant of the spinel $FeAl_2O_4$.

a_0 (Å)	Sample source	Reference	Ref. No.
8.146±0.004[a]	natural crystals, some Mg	Holgersson (1927)	16
8.135±0.002	synthetic powder	Clark, Ally, Badger (1931)	17
8.100±0.002	synthetic powder	Krause and Thiel (1931)	18
8.13	synthetic powder	Tazaki and Kuwabara (1952)	19
8.125±0.002	synthetic powder	Hoffmann and Fischer (1956)	20
8.152±0.001	synthetic powder, 1000°C	Atlas and Sumida (1958)	21
8.150±0.002	synthetic powder, 800°C	Turnock (1958)	22
8.152±0.002	synthetic powder, 1200°C	Roth (1963)	5
8.140±0.001	synthetic single crystals, 1200°C	Slack (present work)	···

[a] 8.155±0.004 Å for pure $FeAl_2O_4$ when corrected for slight amount of $MgAl_2O_4$.

gave an atomic ratio of aluminum to iron of 2.00±0.04. Even though the Al to Fe ratio is exactly 2.00, some of the Fe is probably in the Fe^{3+} state. Such oxidation of the Fe will increase the O to Fe ratio above the ideal value of 4. The chemical analysis of R67 gave this ratio as 4.1±0.1, indicating that some of the Fe was in the Fe^{3+} state. If the O to Fe ratio is actually 4.1, then 20% of the Fe occurs as Fe^{3+}. Except for the possibility that some of the Fe is in the Fe^{3+} state, the present synthetic crystals are close to being ideal $FeAl_2O_4$. A heat treatment of the as-grown crystals is needed in order to reduce the Fe^{3+} concentration to its lowest possible value. Crystal R75 was prepared by taking an as-grown sample of $FeAl_2O_4$, surrounding it with high-purity Al_2O_3 powder, and sealing it inside a capsule of high-purity iron. This capsule was then annealed at 1200°C for 21 h in an effort to bring the volume of the crystal to equilibrium with the reaction[12,21]:

$$FeAl_2O_4 \rightleftarrows Fe + Al_2O_3 + \tfrac{1}{2}O_2.$$

This equilibration produced a slight increase in a_0 to 8.140 ±0.002 Å and, as will be shown later, a noticeable decrease in the optical absorption, and a sharpening of the kink in the thermal conductivity curve at 10°K. Since the equilibration is a diffusion process, annealing times even longer than 21 h may be necessary to bring the bulk of the crystal to equilibrium with the oxygen atmosphere. A thin sample of $FeAl_2O_4$ which was given a longer anneal had a lattice constant of 8.144 Å, which is approaching the ideal value of 8.151 Å. The fact that the a_0 of the synthetic $FeAl_2O_4$ is less than 8.151 Å is attributed to the presence of Fe^{3+}.

Chemical Purity

The chemical purity of the various samples has been measured in order to determine what foreign elements were present. This is especially necessary since many of the samples were natural crystals. The impurity content of samples R42, R54, R56, and R62 has previously been published.[23] The major impurities in the other four samples are listed in Table III. These have been determined by spectrographic analysis in all cases except for the Fe and Cr of R97. These two impurities were determined by aqueous solution colorimetry to ±10%. These results show that Fe is the dominant impurity in R97. Crystal R97 was in fact chosen from a group of several natural spinel crystals just for this reason.

The synthetic $FeAl_2O_4$ is reasonably pure. Most of the impurities appear to have been introduced during the growing process since Johnson-Matthey "Specpure" oxides were used as the starting material. With more care purer samples could be made.

THERMAL CONDUCTIVITY

The physical properties that were measured were the lattice constants a_0 (see Table I), the thermal conductivity, the optical absorption, and the magnetic susceptibility. The interpretation of and the interrelationships between these parameters will be discussed.

Extensive measurements of the thermal conductivity K have been made between 3 and 300°K by techniques previously described.[24] The K versus T curves for R42, R54, R56, and R62 have already been published.[23] They are reproduced again in Fig. 2 along with the new data for the other crystals. The main features to notice in Fig. 2 are the monotonic decrease in K at any and all temperatures with the increasing content of Fe. The pure $FeAl_2O_4$ has the lowest K of all. This crystal is a rare example of a good single crystal with no (or very little) atomic disorder in which the K decreases continuously with decreasing T for all temperatures below 300°K. The other important feature to notice is the "kink" in several of the K versus T curves at 10°K.

TABLE III. Major metallic impurities in several spinel samples in units of 10^{18} atoms/cm^3.

Impurity	Sample R68	Sample R67, R75	Sample R97
Ca	8	<0.7	<5
Cr	<0.2	3	35
Fe	0.4	m[a]	360
Mg	m	0.3	m
Si	2	7	4
Ti	0.5	1	5
V	<0.4	0.3	8
Zn	<0.7	<0.8	20

[a] m = major constituent at a concentration of about 1.5×10^{22} cm^{-3}.

[23] G. A. Slack, Phys. Rev. **126**, 427 (1962).
[24] G. A. Slack, Phys. Rev. **122**, 1451 (1961).

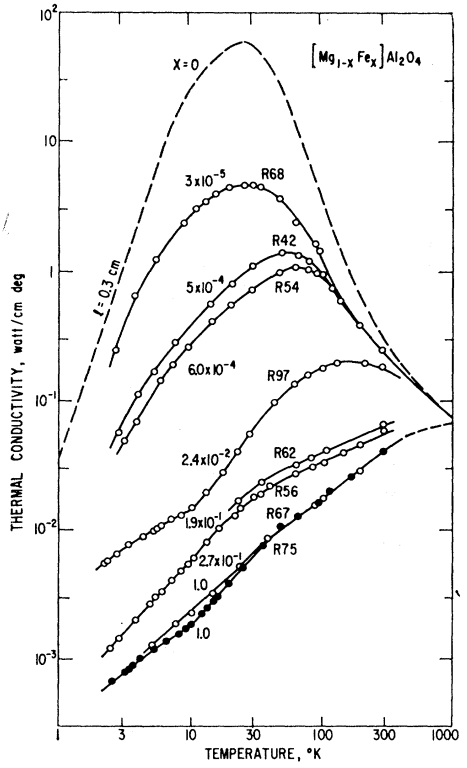

FIG. 2. The thermal conductivity K versus temperature for several mixed crystals of $Mg_{1-x}Fe_xAl_2O_4$. The value of x for each crystal is given. Note the continuous decrease in K with increasing x.

The heat transport in all of these crystals is believed to be caused by phonons. It does not appear that the magnetic moments in any of the crystals become well ordered between 3 and 300°K, so that a magnon heat transport is not at all likely. This lack of ordering will be discussed later. The phonons in the pure $MgAl_2O_4$ with $x=0$ are scattered by[23] the crystal boundaries, the isotopes, and the other phonons for $3°K \leq T \leq 300°K$. The relative strengths of these scattering processes vary with temperature, and their combined effect gives an upper bound to the K given by the dashed curve labeled $x=0$ in Fig. 2. This curve is computed for a specimen diameter of 0.3 cm, which is just the average crystallite size in the purest sample R68. The other crystals ranged in diameter from 0.2 to 0.4 cm, and in length from 0.3 to 1.2 cm. Thus, 0.3 cm is a reasonable average diameter for all of the crystals. Only the purest sample R68 comes close to the K limit imposed by boundary scattering at 3°K.

The failure of sample R68 to have a K as high as the dashed curve in Fig. 2 may be caused by some disorder in the Mg and Al distribution on the A and B sites that has been seen in other synthetic spinels.[4] It may also be caused by the presence of the various chemical impurities listed in Table III. The Fe and Ti are the dominant transition-metal impurities, and are the most likely source of any phonon scattering by the impurities.

In these crystals containing tetrahedral Fe^{2+} it is suggested in this paper that the isolated Fe^{2+} ions are very effective phonon scatterers. The scattering mechanism is believed to be the same as that postulated for Fe^{2+} in the tetrahedral sites in CdTe,[25] and is caused by phonon assisted transition between the several low-lying energy levels of the $3d^6$ configuration. Thus, the phonon scattering and hence the thermal resistivity $W=K^{-1}$ should depend on the Fe^{2+} concentration. Notice that in Fig. 2 for a crystal with $x=0.1$, i.e., somewhere between R97 and R62, the K would decrease monotonically with decreasing T for $T \leq 300°K$. This means that for $x>0.1$, the phonon scattering by the Fe^{2+} predominates over the normal phonon-phonon scattering for all $T \leq 300°K$. In order to characterize the Fe^{2+} scattering mechanism, we are interested in the K as a function of T and of x.

Values of x for the concentration of tetrahedral Fe^{2+} in the various crystals have been obtained from the strength of the optical absorption at 0.60 eV. The details are described later. These x values are given in Table I. The x values for R67 and R75 will change slightly with heat treatment and the residual concentration of Fe^{3+}, however, they are probably between 0.9 and 1.0. Figure 3 shows a plot of the thermal resistivity W versus x at 3, 10, 30, 100, and 300°K for the crystals studied. The straight lines in Fig. 3 are drawn to weight the points for R97 and R75 most heavily since in these two crystals Fe^{2+} is by far the most prevalent impurity. Crystals R62 and R56 have substantial concentrations of Fe^{3+}, as found in the optical absorption studies. Crystals R54 and R68 both have several other impurities whose concentrations are equal to or greater than that of the Fe. Figure 3 indicates, however, that Fe^{2+} is responsible for a major part of the W in these two crystals between 3 and 30°K. The lines in Fig. 3

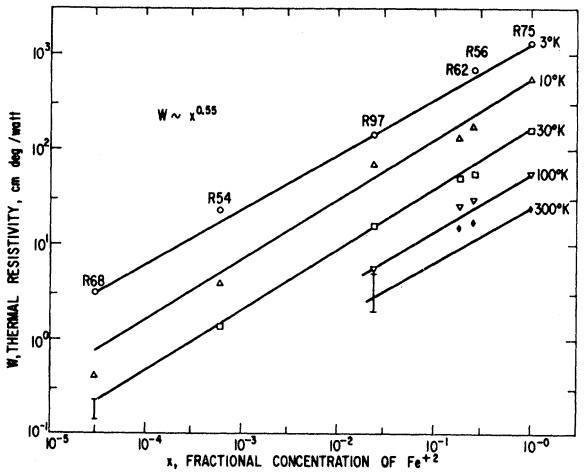

FIG. 3. The thermal resistivity W versus the Fe^{2+} concentration x for several temperatures. For any given temperature, w varies approximately as $x^{0.55}$.

[25] G. A. Slack and S. Galginaitis, Phys. Rev. **133**, A253 (1964).

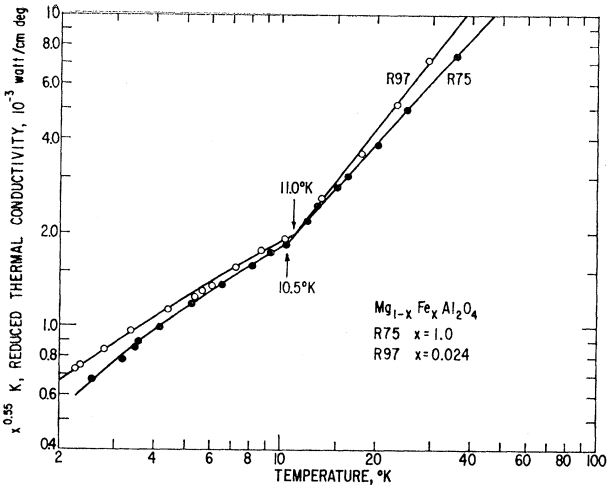

FIG. 4. The reduced thermal conductivity versus temperature in the region of 10°K. The similarity of the "kink" at 11°K for R75 and R97 is quite plain.

show that when the Fe^{2+} is the dominant phonon scatterer, W varies approximately as $x^{0.55\pm0.05}$, or K as $x^{-0.55}$ for all temperatures between 3 and 300°K. The K versus T curves in Fig. 2 show that in the temperature range where Fe^{2+} is the dominant phonon scatterer, K varies roughly as T^{1+}. A detailed calculation of the magnitude, temperature, and Fe^{2+} concentration dependence of K for the crystals shown in Fig. 2 could be made using Callaway's[26] approach if one had a good idea of the relaxation times for phonon scattering by the Fe^{2+} ions and by the normal phonon processes. However, neither is very well known at present. The scattering from the Fe^{2+}, $3d^6$ configuration in tetrahedral sites involves a series of five equally-spaced magnetic levels, and is similar to the case of Fe^{2+} in CdTe.[25] Some recent, preliminary measurements by the author on the optical absorption of crystal R97 at low temperatures places the highest of these 4 excited levels at 120°K above the ground state. If this estimate is correct, the phonon scattering by the Fe^{2+} will be important for temperatures up to a few times 120°K. It is thus not difficult to believe that the Fe^{2+} has reduced the K of $FeAl_2O_4$ at 300°K by a factor of 5 compared to that of $MgAl_2O_4$. The continuous decrease in K with decreasing temperature for $T<300$°K is also not too surprising. The effect of the Fe^{2+} on the K of $FeAl_2O_4$ should disappear only when $T\gg120$°K. From Fig. 2 it appears that the K of $FeAl_2O_4$ and $MgAl_2O_4$ may be nearly equal for $T>1000$°K. A more detailed calculation to explain the $x^{-0.5}$, T^{1+} variation of K is not yet feasible.

The curves for R75 and R97 show that there is some structure in the K versus T curves. Both of these exhibit a decided "kink" or change in slope at 11±1°K. In order to demonstrate the similarity between the two curves, reduced K values for both of them have been replotted side-by-side in Fig. 4. The reduced K is taken as $x^{0.55}$ K in order to correct for different x values. The "kink" for R97 comes at 11±1°K, while that for R75 comes at 10.5±1°K. An average of 11±1°K will be used. For crystal R97 with $x=0.024$ the Fe^{2+} concentration is so small that there is no likelihood of a magnetic A-A interaction between the various Fe^{2+} ions. Thus, in this crystal, each Fe^{2+} ion is scattering the phonons independently of all the other Fe^{2+} ions. Since Fig. 4 shows that the temperature dependence of K is nearly the same for R75 and R97, the conclusion is that the Fe^{2+} ions in R75 are also scattering the phonons independently of one another for $x=1$. It is concluded that the "kink" in the curves in Fig. 4 at 11°K is not produced by any cooperative, long-range magnetic ordering among the A site Fe^{2+} ions in $FeAl_2O_4$, but is produced by some change in the scattering of the phonons from the individual Fe^{2+} ions at 11°K. The K results for R56 in Fig. 3 show a very small "kink" at 11°K, but it is rather weak. The presence of a large amount of Fe^{3+} may be responsible for suppressing the effect.

The question as to whether $FeAl_2O_4$ undergoes a transition to an antiferromagnetic state below 11°K is not completely answered by this result. Roth[5] believes that the magnetic susceptibility data, which will be discussed later, demonstrates the presence of short-range antiferromagnetic ordering below 8 to 10°K. His neutron results, however, fail to show any long-range ordering at these temperatures. The present K results show that if a transition to an antiferromagnetic state does take place in $FeAl_2O_4$, such a transition does not affect the K. This would be surprising in view of the results[24,27,28] on MnO, CoO, MnF_2, and CoF_2; on[29] $CuCl_2\cdot2H_2O$ and $CoCl_2\cdot6H_2O$, and on[30] UO_2, where there was a noticeable break in the K versus T curve on passing through the Néel temperature. More work will be necessary before the 11°K transition in $FeAl_2O_4$ is understood.

As a check on the hypothesis that the Fe^{2+} in the $FeAl_2O_4$ is the cause of the anomalously low thermal conductivity, some measurements of K were made on a single crystal of $CoAl_2O_4$. This crystal R106 is a normal spinel[5] and was grown by E. M. Clausen of this laboratory using a flame-fusion technique. The K results for a crystal 0.83 cm×0.20 cm×0.18 cm annealed in air for 100 h at 1000°C are shown in Fig. 5 together with the curves for $MgAl_2O_4$ (R68) and $FeAl_2O_4$ (R75). The K results for the as-grown $CoAl_2O_4$ sample were identical to those for the annealed sample. Notice that the K values lie between the other two curves except at the

[26] J. Callaway, Phys. Rev. **122**, 787 (1961).

[27] G. A. Slack and R. Newman, Phys. Rev. Letters **1**, 359 (1958).

[28] G. A. Slack, *Proceedings of the International Conference on Semiconductor Physics, Prague, 1960* (Academic Press Inc., New York, 1962), p. 630.

[29] R. H. Donaldson and D. T. Edmonds, Phys. Letters **2**, 130 (1962).

[30] O. Bethoux, P. Thomas, and L. Weil, Compt. Rend. **253**, 2043 (1961).

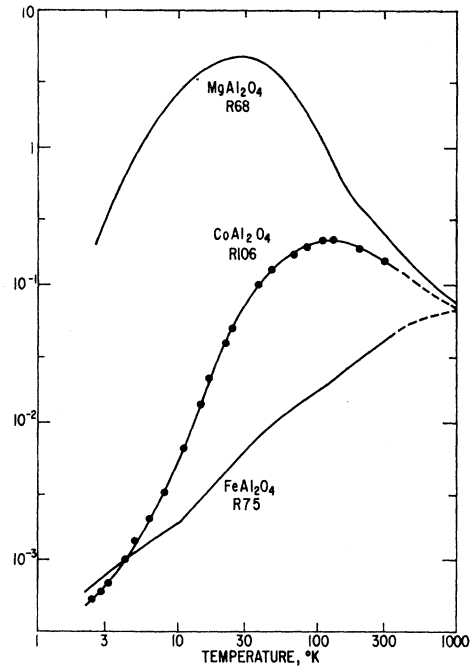

FIG. 5. The thermal conductivity of a single crystal of $CoAl_2O_4$ versus temperature. The results lie between those for $MgAl_2O_4$ and $FeAl_2O_4$, which are also shown.

very lowest temperatures. The K of $CoAl_2O_4$ does not decrease monotonically with decreasing T. All three crystals appear to have nearly identical K for $T \geq 1000$°K. The tetrahedral Co^{2+} has a $3d^7$ configuration, and does not possess[25] any low-lying energy levels in the 1 to 1000°K energy range. Thus it should not scatter phonons with anywhere near the same effectiveness as does the tetrahedral Fe^{2+}. This conclusion is demonstrated by the results in Fig. 5, at least for temperatures between 4 and 300°K. Solely on the basis of the magnetic scattering by the tetrahedral Co^{2+}, the K of $CoAl_2O_4$ should be nearly as high as that of $MgAl_2O_4$. The failure of the $CoAl_2O_4$ to exhibit such a high K may be caused by a partial inversion of the $CoAl_2O_4$, or by other crystal imperfections.

From the differences in K of the spinels $MgAl_2O_4$, $FeAl_2O_4$, and $CoAl_2O_4$, one concludes that the phonon scattering is very sensitive to the details of the magnetic nature of the A-site ions.

OPTICAL PROPERTIES

Optical absorption measurements on most of the samples listed in Table I and on a sample of commercial $MgO \cdot 3.5\ Al_2O_3$ spinel have been made at 300°K over the photon-energy range from 0.1 to 7.0 eV (12- to 0.18-μ wavelength). These measurements were made using three different recording spectrophotometers. A Perkin-Elmer[31] model-421 grating instrument was used from 0.1 to 0.5 eV, and a Beckman[32] DK-2A and a Cary[33] model-14 were used from 0.5 to 7.0 eV. These instruments operated well down to about 1% sample transmission. The sample thickness ranged from 5×10^{-1} to 3×10^{-3} cm. Samples thinner than 3×10^{-3} cm were difficult to prepare because they often broke during the polishing process. This combination of instruments and samples allowed one to measure values of the optical absorption coefficient α from 10^{-1} to 10^{+3} cm^{-1}. The coefficient α is defined by

$$I = I_0(1-R)^2 e^{-\alpha t}, \quad (1)$$

where I_0 = incident light intensity, I = transmitted light intensity, R = reflection loss for a single surface at normal incidence, t = sample thickness in cm.

The two main purposes of these measurements are to determine the site symmetry of the Fe^{2+} in the spinel crystals and to determine the concentration of the Fe^{2+}. The Fe^{2+} in the tetrahedral sites produces a strong absorption in the infrared over a broad band between 0.4 and 0.8 eV. The α-versus-photon energy $h\nu$ curves allow one to make some estimate of the Fe^{2+} and the Cr^{3+} concentration in the crystal.

Reflectivity

Some optical reflectivity measurements were made on $MgAl_2O_4$ and $FeAl_2O_4$ from 0.03 to 2.0 eV in order to identify the regions of strong lattice absorption and to measure the reflection loss R. These measurements were made at 300°K with a Perkin-Elmer[31] model-83 monochromator at nearly normal incidence. The strong lattice peaks were all found in the energy range between 0.03 and 0.11 eV. The samples used were a natural spinel crystal from Burma which was medium-pink in color, and a synthetic crystal of $FeAl_2O_4$ in the as-grown, unannealed condition. The surfaces of the crystals were polished so that they were optically flat before the reflectivity was measured.

The reflectivity results for $MgAl_2O_4$ are shown in Fig. 6. The main lattice absorption peaks are at 0.066 and 0.091 eV. The other smaller peaks that were found are listed in Table IV along with those found for $FeAl_2O_4$. The reflectivity values for $MgAl_2O_4$ in Table IV for normal incidence are reasonably accurate. The values for $FeAl_2O_4$ taken at about 30° from the normal are only approximate, but do indicate the relative strengths of the various peaks. Table V also gives the positions for the absorption maxima by transmission found by other authors[4,34,35] using powdered samples compressed in KBr pellets. The Greek letters serve to identify the various peaks. Even though the peaks in the reflectivity and absorption are not at

[31] Perkin-Elmer Corporation, Norwalk, Connecticut.

[32] Beckman Instruments Inc., Fullerton, California.

[33] Applied Physics Corporation, Monrovia, California.

[34] K. A. Wickersheim and R. A. Lefever, J. Opt. Soc. Am. **50**, 831 (1960).

[35] S. Hafner, Z. Krist. **115**, 331 (1961).

TABLE IV. Reflectivity maxima found for $MgAl_2O_4$ and $FeAl_2O_4$ single crystals.

Designation (a)	$MgAl_2O_4$ (natural) $h\nu$	$\%R$	Character	$FeAl_2O_4$ (synthetic) $h\nu$	$\%R$	Character
α	0.0375 eV	36	sharp peak	0.038 eV	~50	small peak
β	0.059	89	shoulder			
γ	0.066	100	broad peak	0.061	~70	broad peak
δ	0.072	75	shoulder	0.068	~50	weak shoulder
ϵ	0.091	100	sharp peak	0.086	~80	peak
ζ	0.104	50	weak shoulder	0.099	~40	shoulder
θ	0.176	small	see Fig. 7	0.18	low	see Fig. 7

[a] These Greek letters serve only to identify the various peaks.

identical energies, the energies are nearly equal. The strong reflectivity peaks are associated with the strong absorption ones. There is a close similarity between these lattice vibration peaks for $MgAl_2O_4$ and $FeAl_2O_4$ since they both have the spinel crystal structure, and nearly the same lattice constants. The Fe is a heavier atom than the Mg and the reflectivity peaks for $FeAl_2O_4$ occur at an energy about 5% less than those for $MgAl_2O_4$. In the energy range between 0.12 and 3.0 eV (and up to 4 eV actually) the reflectivity R of $MgAl_2O_4$ is quite small (2 to 8%), and there is no structure in the R versus $h\nu$ curve in Fig. 6. The same general statement can be made for $FeAl_2O_4$. Thus, any structure found in the optical transmission curves of the single crystals in this energy range is caused by variations in the absorption coefficient α and the reflection correction is small, see Eq. (1).

Absorption Coefficient

The % transmission curves that were taken were corrected for reflection losses using R values calculated from the refractive index[36,37] n for $MgAl_2O_4$ in the range between 1.6 and 3.0 eV. Beyond these energy limits the calculated R values were extrapolated using the results shown in Fig. 5. The resultant optical absorption coefficients α for the various samples are given in Figs. 7 and 8.

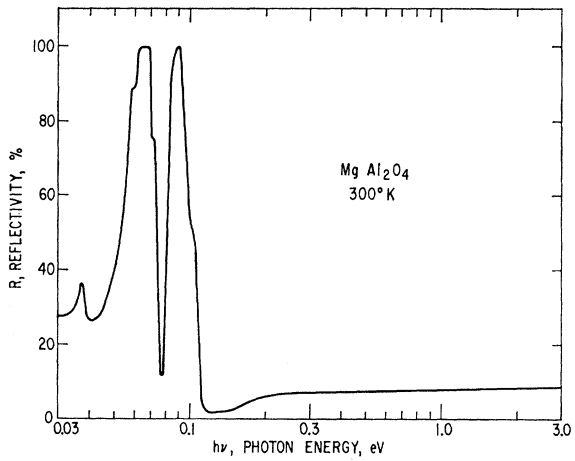

FIG. 6. The optical reflectivity R versus photon energy. These results for a natural single crystal of $MgAl_2O_4$ at 300°K were taken at nearly normal incidence.

1. Pure $MgAl_2O_4$

The highest purity $MgAl_2O_4$ sample R68 in Fig. 7 exhibits an optical window between 0.23 and 6.0 eV. These are the limits at which $\alpha = 1$ cm^{-1}. This synthetic $MgAl_2O_4$ was grown[6] in an atmosphere of hydrogen by diffusing MgO into Al_2O_3. It does not show any signs of the OH or H_2O band at 0.4 eV (3 μ) that has been seen[34,38] in synthetic spinels grown by the flame-fusion process. As a check on the presence of this band a synthetic crystal of MgO+3.5 Al_2O_3 from Linde[39] (crystal R53 of Ref. 23) was measured in this region. It showed a double-peaked band with peaks at 0.415 and 0.436 eV with absorption coefficients of 6 cm^{-1} and 3 cm^{-1}, respectively. For contrast, the R68 crystal had an $\alpha < 0.05$ cm^{-1} in this same energy region. Thus, the 0.4-eV band is not an intrinsic feature of $MgAl_2O_4$, but shows up only in the flame-fusion grown crystals. It has not been seen in any of the natural $MgAl_2O_4$ crystals. It is necessary to understand the source of this band, since the absorption peak for Fe^{2+} ions in the A sites occurs at about this same energy.

TABLE V. Absorption maxima for $MgAl_2O_4$ and $FeAl_2O_4$ powders from the literature.

Designation (a)	$MgAl_2O_4$ (b)	(c)	(d)	$FeAl_2O_4$ (e)
γ	0.0645 eV	0.067	0.065	0.063
δ	0.0716			0.070
ϵ	0.0849	0.086	0.085	0.083
ζ	0.0932	0.092	0.097	
η			0.124	

[a] These Greek letters serve only to identify the various peaks.
[b] Natural $MgAl_2O_4$, Ref. 4.
[c] Synthetic $MgAl_2O_4$, Ref. 35.
[d] Synthetic $MgAl_2O_4$, Ref. 34.
[e] Synthetic $FeAl_2O_4$, Ref. 4.

[36] F. Rinne, Neues Jahrb. Mineral. Geol., Beilageband **58A**, 43 (1928).
[37] K. Schlossmacher, Z. Krist. **72**, 447 (1930).
[38] G. Calingert, S. D. Heron, R. Stair, Soc. Autom. Engin. J. **39**, 448T (1936).
[39] Linde Air Products Company, New York, New York.

2. *Tetrahedral* Fe^{2+}

The main feature in all of the α versus $h\nu$ curves in Figs. 7 and 8 is the very strong absorption band between 0.4 and 0.8 eV. This band is assigned to the tetrahedral Fe^{2+}, $3d^6$ transition $^5E(^5D) \rightarrow {}^5T_2(^5D)$. This same transition has been seen in several II–VI semiconducting compounds doped with Fe. Probably the earliest report of it was by Coblentz[40] in natural crystals of zincblende (cubic ZnS), which almost always contain Fe, where he found a broad single absorption peak at 0.41 eV. Low and Weger[41] have also found this peak in natural zincblende, Pappalardo and Dietz[42] have seen it in Fe-doped synthetic CdS, and the present author[43] has seen it in Fe-doped synthetic CdTe. The energies of the two peaks in this double peak are listed in Table VI. In some cases only a single, broad peak is seen. This absorption peak shifts toward higher energies as the Fe-anion distance decreases, see Table VI.

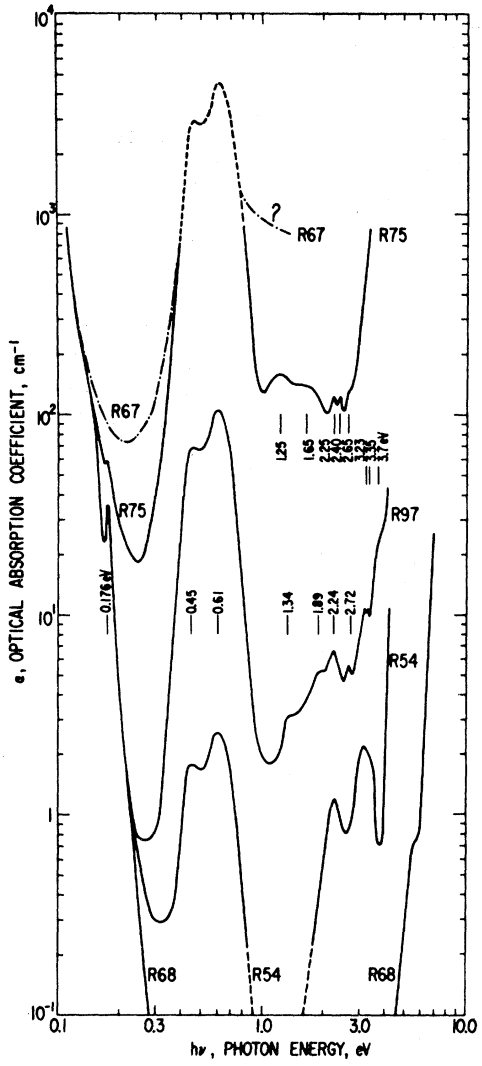

FIG. 7. The optical absorption coefficient α versus the photon energy $h\nu$ for several different single-crystal spinels. Corrections for reflection losses have been made. The energies of various absorption peaks have been labeled in electron volts. The dashed curve for R75 indicates that the absorption between 0.4 and 0.8 eV was too large to be measured. However, the estimated behavior is shown. Similarly the ? for R67 indicates that above 0.8 eV, α was too large to be measured. The main absorption peaks at 0.45 and 0.61 eV are caused by tetrahedral Fe^{2+}.

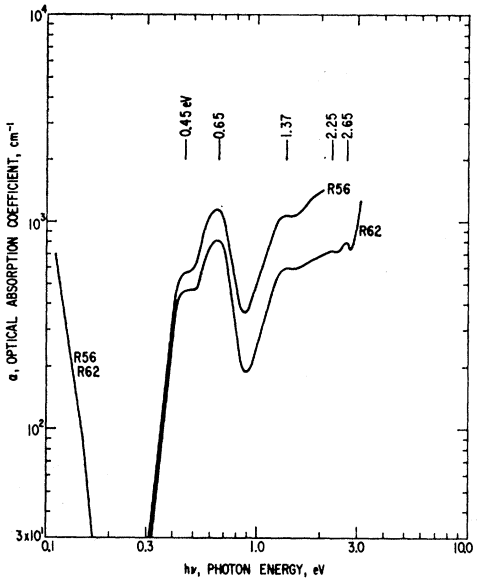

FIG. 8. The optical absorption coefficient α versus the photon energy $h\nu$ for two pleonaste spinels which contain large amounts of both Fe^{2+} and Fe^{3+}. Corrections for reflection losses have been made. The main peaks are labeled in electron volts.

The strength of the electrostatic crystalline field at the Fe^{2+} ion produced by the other surrounding ions is given[44] by the parameter Dq. The energy $h\nu$, at the peak in the α versus $h\nu$ curve is approximately equal to 10 Dq.

TABLE VI. Peak energies for the double-peak, infrared optical absorption band of tetrahedral Fe^{2+} at 300°K.

Crystal	Peaks $h\nu$, eV	Reference	Fe-anion distance, Å
$MgAl_2O_4$, cubic	0.45, 0.61	present work	1.81
ZnS, cubic	0.41	Coblentz[b]	2.34
ZnS, cubic	0.35, 0.50	Low and Weger[c]	2.34
CdS, hex.	0.306, 0.387	Pappalardo and Dietz[d]	2.53
CdTe, cubic	0.34[a]	Slack[e]	2.81

[a] Splits into two peaks when crystal is cooled below 100°K.
[b] See Ref. 40.
[c] See Ref. 41.
[d] See Ref. 42.
[e] See Ref. 43.

[40] W. W. Coblentz, No. 97, Carnegie Institution of Washington, D. C., 1906 (unpublished), Part VI, p. 57.

[41] W. Low and M. Weger, Phys. Rev. **118**, 1119, 1130 (1960).
[42] R. Pappalardo and R. E. Dietz, Phys. Rev. **123**, 1188 (1961).
[43] G. A. Slack (unpublished).
[44] D. S. McClure, in *Solid State Physics*, edited by F. Seitz and D. Turnbull (Academic Press Inc., New York, 1959), Vol. 9, p. 399.

The breadth of the absorption band and the presence of the double peak make the determination of Dq rather inexact. However, an average energy for the two peaks in $MgAl_2O_4$ is 0.53 eV = 4300 cm^{-1} = 10 Dq. So Dq has the not unreasonable value of +430 cm^{-1} for tetrahedral Fe^{2+}. Further understanding of what causes the broadening of the absorption peak will yield a better value of Dq. It is postulated here that the breadth is caused by a strong coupling between these magnetic levels and the lattice vibrations. It is just this coupling which gives rise to the pronounced effects of Fe^{2+} on the thermal conductivity.

3. Other Transition Metal Ions

The other peaks in Figs. 7 and 8 also require some explanation. The small, sharp peak at 0.176 eV has been seen in all of the crystals, and is independent of doping. It is probably a lattice vibration band, and is therefore listed in Table IV. There are numerous peaks between 1.0 and 4.0 eV which vary from sample to sample. Since pure $MgAl_2O_4$, sample R68 has no absorption bands between 0.23 and 6.0 eV, these bands are caused by various transition-metal impurities. So far none of these other bands in Figs. 7 and 8 has been definitely associated with transitions in the tetrahedral Fe^{2+} ion. They all appear to be caused either by octahedral Cr^{3+} in the natural crystals (R54 and R97), by Fe^{3+}, or by octahedral Fe^{2+} in the other crystals. The various Cr^{3+} peaks in R54 and R97 are dealt with in the Appendix. The conclusion is that except for the 1.34-eV peak in R97 all the other peaks above 1.0 eV in these two crystals are due to Cr^{3+}. Crystal R54 shows the two peaks at 2.24 and 3.23 eV characteristic of octahedral Cr^{3+}. In R97 the simple octahedral Cr^{3+} spectrum has been modified by the presence of the much larger concentration of tetrahedral Fe^{2+}.

4. Other Fe Ions

Let us now consider the possibilities involved in the absorption spectra of Fe^{3+}, both octahedral and tetrahedral, and of octahedral Fe^{2+}. If $FeAl_2O_4$ were a perfectly stoichiometric, normal spinel, then only tetrahedral Fe^{2+} would exist. The x-ray data have shown[1,2] that $FeAl_2O_4$ is a normal spinel. The recent work of Schmalzried[45] on other aluminates has shown that $CoAl_2O_4$ is nominally a normal spinel, but when equilibrated at 1000°C is partially inverse. In view of the similarity of the octahedral preference energies of $CoAl_2O_4$ and $FeAl_2O_4$ calculated by Miller,[46] $FeAl_2O_4$ can be expected to be slightly inverse in the 1000 to 1500°C range. From neutron scattering data, Roth[5] has found that in his powder sample of synthetic $FeAl_2O_4$, annealed at 1200°C, about 15% of the iron was in the octahedral sites. Thus there will probably be some small amount (i.e., 1 to 20%) of octahedral Fe^{2+} in the present single crystals annealed at 1200°C. The presence of Fe^{3+} in the $FeAl_2O_4$ is less certain. It is well known[14] that the iron in wüstite or "FeO" cannot be reduced to the point where all of the iron is divalent. Thus, one might expect some Fe^{3+} in the $FeAl_2O_4$ even when it is at the low-oxygen pressure dissociation limit of decomposing into Fe, Al_2O_3, and O_2. From Miller's[46] calculations one would predict that this Fe^{3+} would be on the tetrahedral sites. Notice that any octahedral Fe^{3+} that is present requires only that one of the many tetrahedral Fe^{2+} ions in the $FeAl_2O_4$ transfers an electron to the octahedral Fe^{3+} in order to yield an octahedral Fe^{2+} and a tetrahedral Fe^{3+} ion. For example, this exchange is quite favorable in Fe_3O_4, which is an inverse spinel where the Fe^{3+} is on the tetrahedral sites in competition with Fe^{2+}. The opposite conclusion of Hoffman and Fischer[20] that the first small additions of Fe^{3+} go into the octahedral sites is suspect since their lattice constants at low Fe_3O_4 concentrations do not agree with the later ones of Atlas and Sumida[21] or of Turnock.[22] It seems probable that at low concentrations of Fe^{3+} in $FeAl_2O_4$ the Fe^{3+} occurs on the tetrahedral sites. Therefore, in the interpretation of the optical absorption spectra of the mixed $FeAl_2O_4$–$MgAl_2O_4$ crystals, it is necessary to consider tetrahedrally and octahedrally coordinated Fe^{2+}, and tetrahedrally coordinated Fe^{3+}.

The optical absorption caused by octahedral Fe^{2+} is believed to be the cause of the broad peaks seen in Fig. 6 for R75 at 1.23 and 1.65 eV. Previous work by Holmes and McClure[47] has shown that hydrated, octahedral Fe^{2+} in $FeSO_4 \cdot 7H_2O$ crystals possesses only two rather weak, broad absorption bands at 1.04 and 1.34 eV in the energy range from 0.75 to 4.7 eV, with a combined oscillator strength of $f \simeq 4 \times 10^{-5}$. These authors also found that the absorption of Fe^{2+} in water solution was very similar. The method of calculating the oscillator strengths f from the optical absorption curves is that given by Dexter.[48] Octahedrally coordinated Fe^{2+} is a well-known colorant in glass,[49] where it produces an absorption band at about 1.2 eV (1 μ) in the infrared. Octahedral Fe^{2+} in MgO was found by Low and Weger[41] to have a broad, poorly defined absorption peak at 1.24 eV.

A study of the optical absorption of Fe^{2+} in MgO by the present author[43] shows, that in the energy range between 0.5 and 3.0 eV, there is a broad, rather weak, double-peaked absorption band with peaks at 1.21 and 1.46 eV. The derived oscillator strength is $f \simeq 6 \times 10^{-5}$ for each peak,[6] close to the value for the hydrated Fe^{2+}. The energies for these absorption bands of Fe^{2+} in MgO and $FeSO_4 \cdot 7H_2O$ are in reasonable agreement with the

[45] H. Schmalzried, Z. Physik. Chem. (Frankfurt) **28**, 203 (1961).
[46] A. Miller, J. Appl. Phys. **30**, 245 (1959).
[47] O. Holmes and D. S. McClure, J. Chem. Phys. **26**, 1686 (1957).
[48] D. L. Dexter, in *Solid State Physics*, edited by F. Seitz and D. Turnbull (Academic Press Inc., New York, 1958), Vol. 6, p. 353, 371.
[49] W. A. Weyl, *Coloured Glasses* (Society of Glass Technology, Sheffield, 1951), Chap. 7.

1.23- and 1.65-eV bands seen in $FeAl_2O_4$ in Fig. 6. This is the reason for the assignment of these two bands to octahedral Fe^{2+}. If one makes the assumption that 15% of all the Fe^{2+} in the R75 sample of $FeAl_2O_4$ is on the octahedral sites, and is producing the 1.23-eV band, Fig. 6, the calculated oscillator strength for this 0.7-eV wide band is $f \simeq 3\times10^{-4}$. This is five times higher than that found for MgO. Since the actual concentration of octahedral Fe^{2+} in R75 may be higher or lower than the 15% found by Roth, the f value is only approximate. If anything, the octahedral Fe^{2+} concentration in R75 is probably less than 15% of the total, thus making $f>3\times10^{-4}$. The optical transition responsible for this broad, double-peaked band is believed to be the lowest energy one possible,[44] that is $^5T_2(^5D) \rightarrow {}^5E(^5D)$. The intensity of this optical transition and hence its f value is enhanced by distortion of the local cubic symmetry around the Fe^{2+} ion. The f value is small in highly symmetric environments such as at a Mg site in MgO. In $FeAl_2O_4$ the oxygen ions surrounding the octahedral site form a distorted octahedron. The site symmetry may be further reduced by the presence or absence of an Al^{3+} ion in one or more of the surrounding tetrahedral sites in the real crystal. These sites would, of course, be occupied only by Fe^{2+} in the pure, normal spinel. These effects will all serve to make the oscillator strength f of octahedral Fe^{2+} in $FeAl_2O_4$ greater than it is in MgO. Therefore, the optical absorption data is not yet of much help in determining the absolute concentration of octahedral Fe^{2+}, and hence the fractional inversion in $FeAl_2O_4$. However, it seems clear that the 1.23- and 1.65-eV bands are caused by octahedral Fe^{2+}, and may be useful in determining changes in the fractional inversion.

The other absorption peaks seen for R56 and R62 in Fig. 7 above 1 eV and for R75 in Fig. 6 above 2 eV are probably associated with the Fe^{3+} ions. Just what the assignments should be are rather uncertain. The lowest energy peak for Fe^{3+} in octahedral coordination with oxygen in α-Fe_2O_3 has been found by Bailey[50] at 1.49 eV. A similar peak at the same energy in $Y_3Fe_5O_{12}$(YIG) has been found by Dillon.[51] This is probably the $^6A_1(^6S) \rightarrow {}^4T_1(^4G)$ transition. The first transition for tetrahedral Fe^{3+} should be at an even higher energy since Fe^{3+} has a ^6S ground state and the crystalline field at a tetrahedral site is about half of that at an octahedral site. Therefore, the optical absorption characteristic of tetrahedral Fe^{3+} should occur for $h\nu>1.5$ eV in these oxide spinels. The optical absorption of Fe^{3+} tetrahedrally coordinated by Cl^{-1} ions has been studied by Friedman.[52] He found a number of peaks starting at 1.7 eV and extending toward higher energies. It seems reasonable to suppose that the 2.25-, 2.40,- and 2.65-eV peaks in R56, R62, and R75 may be caused by tetrahedral Fe^{3+}. More work is clearly necessary before such an assignment is convincing.

5. *Charge Transfer*

The last feature of Figs. 7 and 8 that remains unexplained is the hump in the curves for samples R56, R62, and R97 at 1.35 eV. Samples R56 and R62 have fairly large concentrations of Fe^{3+} ions in them, as will be shown later. These Fe^{3+} ions are probably on tetrahedral sites, as are the more numerous Fe^{2+} ions. When the same cation in two different charge states exists on the same lattice site in a crystal, it is relatively easy for a photon to cause an electron transfer between the two differently charged ions. Such a process is believed to be the source of a rather broad, structureless absorption in NiO,[53] $Y_3Fe_5O_{12}$,[54] and Fe_3O_4.[55] It is suggested here that this charge transfer absorption commences at about 1.35 eV in the present spinel crystals, and accounts for the hump in the curves. It would then be responsible for the dull, yellowish-brown appearance of the pleonaste spinels, R56 and R62, by transmitted light. See Table I.

CONCENTRATION OF TETRAHEDRAL Fe^{2+}

The shape of all of the absorption curves in Figs. 7 and 8 between 0.3 and 0.9 eV is nearly the same. The absorption in this portion of the curve is caused by the presence of tetrahedral Fe^{2+}. Since the shapes are all similar, the value of α at, say, the 0.61-eV peak should be proportional to the concentration of tetrahedral Fe^{2+}. The Fe concentration in R97 has been carefully measured as $3.6\pm0.4\times10^{20}$ atoms/cm^3. Since there is no sign of any optical absorption due to octahedral Fe^{2+}, and since the 1.34-eV peak, which is the only peak that might be associated with the presence of Fe^{3+}, is very weak, it is concluded that tetrahedral Fe^{2+} is by far the dominant species of Fe in crystal R97. The peak absorption cross section σ_p is defined by

$$\sigma_p=\alpha_p N^{-1}, \qquad (2)$$

where α_p=absorption coefficient at the peak, and N=concentration of the absorbing ions. The computed value is $\sigma_p=2.9\times10^{-19}$ cm^2 for the 0.6-eV peak in R97. From Fig. 7 the full width of the 0.6-eV peak at $\alpha=0.5\alpha_p$ is 0.22 eV. This width and the value of σ_p of 2.9×10^{-19} cm^2 yields[48] an oscillator strength of $f=4\times10^{-4}$. The 0.45-eV peak gives a somewhat smaller calculated value of $f=1\times10^{-4}$.

The concentration of tetrahedral Fe^{2+} in the other crystals in Figs. 7 and 8 has been calculated on the assumption that tetrahedral Fe^{2+} concentration is proportional to α_p at 0.6 eV. The results are given in Table VII along with the total concentration of Fe

[50] P. C. Bailey, J. Appl. Phys. **31**, 39S (1960).
[51] J. F. Dillon, J. Phys. Radium **20**, 374 (1959).
[52] H. F. Friedman, J. Am. Chem. Soc. **74**, 5 (1952).
[53] R. Newman and R. M. Chrenko, Phys. Rev. **114**, 1507 (1959).
[54] R. A. Lefever and A. B. Chase, J. Chem. Phys. **32**, 1575 (1960).
[55] W. E. Engeler (private communication).

TABLE VII. A comparison of the concentration of tetrahedral Fe^{2+} ions (optical) with the concentration of total Fe (chemical).[a]

Sample	Conc. tetra. Fe^{2+} atoms/cm^3	Conc. Fe total atoms/cm^3	x
R68	$<5\times10^{17}$	4×10^{17} s	3×10^{-5}
R54	0.9×10^{19}	2×10^{19} s	6.0×10^{-4}
R97	3.6×10^{20} a	3.6×10^{20} w	2.4×10^{-2}
R62	2.7×10^{21}	5.0×10^{21} w	1.9×10^{-1}
R56	4.0×10^{21}	6.2×10^{21} w	2.7×10^{-1}
R67, R75		1.5×10^{22} w	~1

[a] a = assumed to be identical to concentration of total iron. s = determined from an emission spectrograph to within a factor of two. w = determined from a wet chemical analysis to $\pm10\%$. x = fraction of tetrahedral sites occupied by Fe^{2+}.

determined chemically. For the $FeAl_2O_4$ crystal the absorption was too large to be measured, and the expected curve, shown dashed in Fig. 7 between 0.4 and 0.8 eV, has been estimated from the chemical determination. The agreement with the known portion of the curve is quite good, showing that the proportionality assumption is not too bad. In Table VII the agreement between the optical and chemical values for R68 and R54 is again satisfactory. However, for samples R62 and R56 the chemical concentration is higher than the concentration of tetrahedral Fe^{2+}. Judging from the chemical analyses of these samples in Ref. 23 and the optical absorption curves in Fig. 8, the remaining 40% of the Fe probably occurs as Fe^{3+}.

MAGNETIC SUSCEPTIBILITY

The magnetic sysceptibility χ of an as-grown single crystal of $FeAl_2O_4$ quite similar to sample R67 was measured from 1.9 to 290°K. The measurements were made by Kouvel and Hartelius with an apparatus[56]

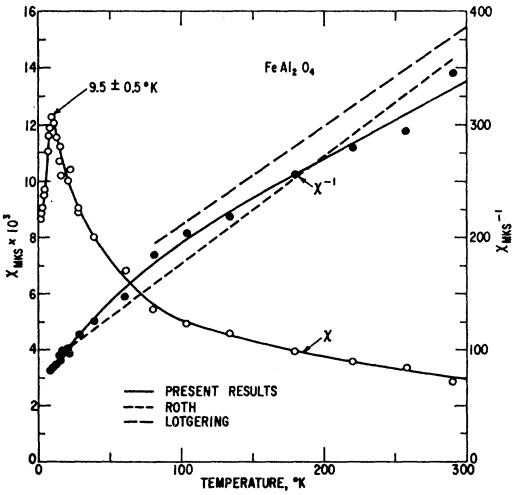

FIG. 9. The magnetic susceptibility χ and its reciprocal χ^{-1} versus temperature for a single crystal of $FeAl_2O_4$ similar to R67. The χ^{-1} curves obtained by other authors for powder samples are also shown.

[56] J. S. Kouvel, C. D. Graham, Jr., and J. J. Becker, J. Appl. Phys. **29**, 518 (1958).

described previously. The susceptibility was independent of applied field for values of the magnetic field H, between 1.5×10^5 to 8×10^5 A/m. (2000 to 10 000 Oe.) The susceptibility in rationalized mks units is shown in Fig. 9. The susceptibility is defined as the ratio of the induced magnetic moment per unit volume (A/m) to the applied magnetic field (A/m), and is dimensionless. These χ values can, if desired, be converted to emu/cm^3 by dividing by 4π. The x-ray density of $FeAl_2O_4$ is 4.26 g/cm^3. There is a very sharp peak in the χ versus T curve at 9.5 ± 0.5°K. The χ^{-1} curve for the single crystal above 9.5°K is also shown in Fig. 9 compared with the recent data of Roth[5] and Lotgering[57] on powder samples. The present results lie between these two previous curves, and indicate that the χ is somewhat dependent on the exact nature of the sample. Small changes in the fractional inversion and the Fe^{3+} content are probably responsible for the variability in χ above 10°K. They are presumably responsible for slight shifts in the peak temperature. Roth[5] found a peak at 8°K. These measurements have not yet been made on annealed single crystals similar to R75.

The 9.5°K temperature for the peak in the χ versus T curve closely matches the "kink" in the K versus T curve at 11 ± 1°K. It would seem that these two features are closely related. Since the "kink" in the K curve appears to be independent of the Fe^{2+} concentration, it is postulated here that the position of the peak may also be nearly independent of the Fe^{2+} concentration. Thus the behavior of the χ versus T curve may be a function of the individual Fe^{2+} ions, and may not be associated with a long-range ordering of the magnetic moment of the Fe^{2+}. A localized Jahn-Teller distortion of the Fe^{2+} ions at 11°K could, perhaps, account for much of the observed behavior. It is known that the normal spinel $FeCr_2O_4$ undergoes[58–60] such a distortion at 135°K, which is rather higher than its Curie temperature[58,61] of about 85°K. Even though Roth[5] found no evidence for a crystallographic distortion in the cubic $FeAl_2O_4$ at 4°K, it is possible that there is a small, local distortion around each Fe^{2+} site. This local distortion, however, may not be large enough to produce a long-range, cooperative, crystallographic distortion. The neutron scattering results of Roth also failed to show any evidence of long-range ordering in $FeAl_2O_4$ at 4°K. This rather unusual behavior of tetrahedral Fe^{2+} may be associated with the four low-lying energy levels, the closest of which is about 30°K above the singlet ground state. Since the ground state is a singlet with no orbital or spin degeneracy, the Fe^{2+} should have no magnetic moment in zero magnetic fields at temperatures well below 30°K. Thus, one might

[57] F. K. Lotgering, Phys. Chem. Solids **23**, 1153 (1962).
[58] C. H. Shomate, Ind. Eng. Chem. **36**, 910 (1944).
[59] E. Whipple and A. Wold, J. Inorg. Nucl. Chem. **24**, 23 (1962).
[60] A. Wold, R. J. Arnott, E. Whipple, and J. B. Goodenough, J. Appl. Phys. **34**, 1085 (1963).
[61] F. K. Lotgering, Philips Res. Rept. **11**, 190 (1956).

expect that signs of a magnetic ordering at these temperatures would not occur. It would appear desirable to make χ measurements on mixed crystals of $FeAl_2O_4$–$MgAl_2O_4$ in order to test some of these speculations. This has not yet been done.

CONCLUSIONS

(1) A method of growing good single crystals of $FeAl_2O_4$ has been devised. A post-growth heat treatment in the appropriate atmosphere permits some control of the concentration of the residual Fe^{3+} and the fractional inversion.

(2) The thermal conductivity K of synthetic crystals of $FeAl_2O_4$ and $MgAl_2O_4$ and natural crystals of $Mg_{1-x}Fe_xAl_2O_4$ has been measured from 3 to 300°K. At all temperatures, the K decreases with increasing Fe^{2+} concentration x for $0 \leq x \leq 1$. For $x=1$, the K exhibits the unusual behavior of decreasing continuously with decreasing temperature for $T \leq 300$°K. In all of the crystals the heat is transported by phonons.

(3) The phonon scattering from the tetrahedral Fe^{2+} is quite strong. This scattering produces a change in the slope of the K versus T curve at 11 ± 1°K, independent of the Fe^{2+} concentration. These results suggest that the anomaly at 11°K is associated with the individual Fe^{2+} ions, and is not caused by the occurrence of an antiferromagnetic state.

(4) The magnetic susceptibility χ of a single crystal of $FeAl_2O_4$ has been measured from 1.9 to 290°K. The χ versus T curve shows a peak at 9.5 ± 0.5°K, in reasonable agreement with the 11°K peak found from the K measurements. It is suggested that this behavior may be characteristic of tetrahedral Fe^{2+}, and is not to be associated with the onset of an antiferromagnetic state.

(5) Thermal conductivity measurements on $CoAl_2O_4$ show that tetrahedral Co^{2+} is not as effective a scatterer of phonons as is tetrahedral Fe^{2+} in the range from 4 to 300°K.

(6) The optical absorption coefficients of crystals of $Mg_{1-x}Fe_xAl_2O_4$ for $0 \leq x \leq 1$ have been measured at 300°K for photon energies between 0.1 and 7.0 eV. The tetrahedral Fe^{2+} produces a broad, double-peaked absorption band between 0.4 and 0.6 eV. This absorption band has been used to measure the value of x.

Additional optical absorption bands have been seen which are due to octahedral Fe^{2+} and octahedral Cr^{3+}.

ACKNOWLEDGMENTS

I wish to thank J. H. McTaggart for his aid in growing the crystals and in making many of the measurements, R. M. Chrenko for his assistance with the optical absorption and reflectivity measurements, and Dr. J. S. Kouvel and C. C. Hartelius for measuring the magnetic susceptibility. I also thank E. M. Clausen for the $CoAl_2O_4$ crystal. My thanks are extended to W. Roth and F. S. Ham for several fruitful discussions concerning the nature of $FeAl_2O_4$.

APPENDIX: THE OPTICAL ABSORPTION OF Cr^{3+} IN $MgAl_2O_4$ SPINELS

Almost all natural crystals of $MgAl_2O_4$ contain traces of Cr. The chemical analyses in Table III and Ref. 23 show that Cr is indeed present in the natural crystals R54, R56, and R97. The Cr^{3+} ion has a very strong preference[46] for the octahedral sites in the spinel, and thus occurs only in these sites in $MgAl_2O_4$. The optical absorption of Cr^{3+} in spinel has been studied by many people,[62–71] and at low concentrations in natural crystals of reasonably pure $MgAl_2O_4$ it gives rise to two broad, intense absorption bands at 2.25 and 3.21 eV. Crystal R54 in Fig. 7 shows these two bands with the peaks at 2.30 and 3.18 eV, in good agreement with the previous literature. The emission spectrographic analysis of this sample showed a Cr content of 2×10^{19} cm^{-3} to within a factor of, say, 2. The calculated oscillator strengths[48] are, to within a factor of 2, $f = 2 \times 10^{-4}$ and 5×10^{-4} for the 2.30- and 3.18-eV peaks, respectively. If the synthetic crystal containing a nominal 0.5 weight % Cr studied by Schlossmacher is considered, the derived f value for his 2.21-eV peak is $f = 0.9 \times 10^{-4}$ to within a factor of 2. Thus the assignment of the 2.30-eV peak in R54 to Cr^{3+} is reasonable in terms of both the photon energy and the magnitude of the absorption coefficient. The optical absorption from a known amount of Cr^{3+} in α-Al_2O_3 has been measured by Maiman *et al.*[72] Their results for the 2.23- and 3.02-eV absorption bands averaged over the three directions in the crystal give f values of approximately 2×10^{-4} and 6×10^{-4}, respectively, for the two bands. These results for α-Al_2O_3 are in very good agreement with those for $MgAl_2O_4$. Of the other various references already cited for Cr^{3+} in $MgAl_2O_4$, none have enough data to enable a calculation of the oscillator strengths to be made.

Let us now consider the various bands found in R97 between 1.5 and 4.0 eV. The 2.24-eV band and the double-peaked band at 3.23 and 3.35 eV are believed to be the two Cr^{3+} bands that appear prominently in R54. The chemical analysis of R97 gave a Cr content of $3.5 \pm 0.3 \times 10^{19}$ cm^{-3}. From this value the calculated oscillator strengths are $f = 8 \times 10^{-4}$ for the 2.24 eV and $f = 16 \times 10^{-4}$ for the "3.29-eV" band. These f values are about 3 times larger than before. These two bands are

[62] O. Weigel, Neues Jahrb. Mineral. Geol., Beilageband **48**, 274 (1923).
[63] O. Weigel and H. Ufer, Neues Jahrb. Mineral. Geol., Beilageband **57A**, 397 (1928).
[64] K. Schlossmacher, Z. Krist. **72**, 447 (1930).
[65] K. Schlossmacher, Z. Krist. **75**, 399 (1930).
[66] K. Schlossmacher and I. Meyer, Z. Krist. **76A**, 377 (1931).
[67] O. Deutschbein, Ann. Phys. **14**, 712, 729 (1932).
[68] E. Kolbe, Neues Jahrb. Mineral. Geol., Beilageband **69A**, 183 (1934).
[69] O. Schmitz-Dumont and D. Reinen, Z. Electrochem. **63**, 978 (1959).
[70] R. A. Ford and O. F. Hill, Spectrochim. Acta **16**, 1318 (1960).
[71] A. Neuhaus, Z. Krist. **113**, 195 (1960).
[72] T. H. Maiman, R. H. Hoskins, I. J. D'Haenens, C. K. Asawa, and V. Evtuhov, Phys. Rev. **123**, 1151 (1961).

TABLE VIII. Comparison of the optical absorption transitions of Cr^{3+} in $MgAl_2O_4$ with those of $[Cr(H_2O)_6]^{3+}$.

Transition	Energy, $h\nu$, in eV R54	R97	$[Cr(H_2O)_6]^{3+}$
$^4A_2(^4F) \rightarrow {}^2E(^2G)$		1.89	1.85
$\rightarrow {}^2T_1(^2G)$			1.87
$\rightarrow {}^4T_2(^4F)$	2.30	2.24	2.23
$\rightarrow {}^2T_2(^2G)$		2.72	2.60
$\rightarrow {}^4T_1(^4F)$	3.18	3.23, 3.35	3.05
$\rightarrow {}^2A_1(^2G)$		3.7	
$\rightarrow {}^4T_1(^4P)$			4.64

also assigned to Cr^{3+}, and their f values, though larger, are reasonable. The somewhat larger f values are thought to be caused by the presence of the Fe^{2+} in the tetrahedral sites enhancing the transition probabilities of the Cr^{3+} in the octahedral sites. The chemically determined concentration of Fe in R97 is $(3.6\pm0.3)\times10^{20}$ cm^{-3}. Thus, 1 out of every 42 tetrahedral sites is occupied by Fe. Since each tetrahedral site in the spinel lattice has 12 nearest octahedral sites, there will be 4.3×10^{21} cm^{-3} octahedral sites, or 1/7 of the total which have an Fe atom as a next-nearest neighbor. If the Cr atoms are randomly distributed over the octahedral sites, then 1/7 of them will be affected by the presence of the tetrahedral Fe in R97. For low concentrations of Fe and Cr the fraction of the Cr sites that are paired with Fe is proportional to the Fe concentration. The fraction of the Cr sites in R54 that are paired is 0.004. The optical absorption spectrum of the Cr^{3+} in R54 is thus not influenced by the presence of the Fe^{2+}. In R97 the case is different. The absorption of the 2.24 and "3.29" eV bands is apparently enhanced. Also the "3.29" eV band has been split into two components, as mentioned previously. In addition there are 3 normally very weak octahedral Cr^{3+} peaks which show up in Fig. 7 as absorption bands at 1.89, 2.72, and a shoulder at 3.7 eV. The 1.89- and 2.72-eV bands have been seen before in blue or blue-green, natural spinel crystals[64,68] which are known[66] to contain Fe^{2+}. The 3.7-eV band has been seen before by Weigel[63] in synthetic $MgAl_2O_4$ containing Cr^{3+}. The assignment of these several bands to various known transitions in octahedral Cr^{3+} is given in Table VIII. The corresponding energies found for $[Cr(H_2O)_6]^{3+}$ are also shown.[73] The agreement is good, indicating that the several absorption bands in R97 between 1.5 and 4.0 eV are caused by the Cr^{3+}. None of them can be attributed directly to optical transitions within the d shell of the tetrahedral Fe^{2+}. This is in contrast to the suggestions of Schlossmacher[64–66] who believed that the absorption spectrum in the visible range of the Fe containing $MgAl_2O_4$ crystals was actually due to the Fe^{2+}. In his crystals as in R97, it is caused by the presence of Cr^{3+}. The Fe^{2+} has, however, strongly modified the Cr^{3+} absorption spectrum. The absorption band at 1.34 eV in R97 is at too low an energy to be caused by the octahedral Cr^{3+}. As explained before, it is believed to be associated with the presence of some tetrahedral Fe^{3+}.

[73] Y. Tanabe and S. Sugano, J. Phys. Soc. Japan 9, 766 (1954).